JETS IN MINIMUM BIAS PHYSICS

G.Pancheri*
Physics Department, Harvard University, Cambridge,Mass.02138 ,USA
and
INFN, Laboratori Nazionali di Frascati, P.O.Box 13, Frascati,Italy

Y.Srivastava
Physics Department,Northeastern University,Boston,USA

Abstract

We discuss and present phenomenological evidence to support the hypothesis that several new phenomena observed in low p_t physics are due to the presence of low-x QCD jets in minimum bias physics. The phenomena we examine are KNO scaling violations, growth of $< p_t >$ with multiplicity and rise of the non- single diffractive part of the total cross-section.

(*) Supported in part by NSF PHY-82-15249 and DOE DEACO276ERO3064

1. Introduction

We discuss here the hypothesis that many new phenomena observed in low p_t physics at the collider have as a common origin the emergence of QCD jets,which can be a visible component of the cross section in minimum bias physics. In what follows, we shall first illustrate the motivation for this suggestion[1], then we shall describe a simple model which shows how to relate KNO scaling violations[2] to the multiplicity dependence of $< p_t >$ for single particle inclusive distributions[3]. Next we will comment upon the energy dependence of the jet-cross section and compare it with the presently observed $\log^2 s$ growth of σ_{tot}[4]. To test the hypothesis that minimum bias physics is being affected in a "macroscopic" way by QCD jets , we suggest to study the transverse energy distribution of minimum bias events and try to separate the mini-jet contribution from the bulk of many-parton interactions. A calculation of transverse energy distribution which takes into account the structure of the underlying event is proposed.

2. Motivation

Several anomalous effects have been observed in low p_t physics as the available energy increased from $\sqrt{s} = 30\ GeV$ to $540\ GeV$. Some of these effects were already observable at the ISR[5], but it was at the CERN collider that the data fully confirmed the previous trend. These effects include :

(i) KNO scaling violations ;
(ii) rise of the non-single diffractive part of the total cross section ;
(iii) growth of $< p_t >$ with multiplicity .

Other possible effects are the rise of the central plateau[6] and hence the $\log^2 s$ type increase of the average multiplicity $< n >$[7]. It is expected that new data to be collected shortly up to $\sqrt{s} = 900\ GeV$ will confirm the observed behaviour. Figure 1 shows some of these effects. In fig.(1a), we show the energy dependence of the moments C_q of the KNO function, where

$$C_q = \int z^q \Psi(z) dz \qquad\qquad z = \frac{n}{< n >}$$

and the KNO function is defined as

$$\Psi(\frac{n}{< n >}) = < n > \frac{\sigma_n}{\sum_n \sigma_n}$$

The lower energy prediction [8]that the shape of the KNO function should remain constant with energy is clearly violated at the collider, where the KNO moments, roughly constant at lower energies, can be seen to depart from the ISR value. Such deviations are particularly noticeable for the high moments (large q). This indicates that the scaling violations are mostly in the high multiplicity region, i.e. at large n. Fig.(1b) shows the well known behaviour of the total cross-section, which rises by about 50% from its lowest ISR value[9] to the value presently measured by both UA4 and UA1 collaborations. Finally,in Fig.(1c) one can see the growth of $< p_t >$ with multiplicity which characterizes the single particle inclusive distributions and which had already been observed in cosmic ray physics[10] a few years before being measured at the collider. Each of the phenomena described

above has received a variety of interpretations[11], ranging from the emergence of quark-gluon plasma [12]to increase of central region collisions[13,14,15]. The point must be made however that all of the above data show violations from the $\log s$ type behaviour which dominated low energy physics through FNAL and ISR. The most appealing explanation of the above phenomena is that QCD parton-parton scattering are responsible for such "scaling violations" and we suggest that a full program be started to verify this hypothesis both experimentally and phenomenologically. Experimentally, an attempt must be made to separate low-E_t jets from the minimum bias sample and study, for each separate sample, the multiplicity distribution as well as the p_t distribution as a function of the multiplicity. An effort in this direction has started and has been reported at this conference[16]. A sample of 40k m.b. events was analyzed with the standard UA1 jet finding algorithm applied to the calorimeter information (jet axis : $|\eta| < 1.5$). The events were then divided into two data samples: the "jetty" events characterized by the presence of at least one jet of energy $\geq 5\ GeV$ and the "non-jetty" events, to which the remaining events belonged. Preliminary findings can be summarized as follows :

(i) a large fraction of m.b. events exhibits *jet activity*, i.e. $\approx 12 \div 15\%$ of the sample has at least one jet with $E_T \geq 5\ GeV$.

(ii) the uncorrected inclusive cross-section extrapolates nicely to the standard high E_T data ;

(iii) the two classes of events exhibit remarkable differences:

- different $< n_{ch} >$ ($|\eta| < 2.5$) :
  $< n >_{no-jets} = 15$
  $< n >_{jetty} = 35$
- different KNO distributions
- for events with jet(s), $< p_t >$ is independent of the multiplicity and larger than the one for the non-jetty eventts
- the transverse energy distribution accompanying the two samples is different and is characterized by

$$< E_T >_{jetty} \approx 2\ < E_T >_{no-jet}$$

In figs.2 and 3 we show some of the results of this preliminary UA1 analysis of 1983 data. In fig.(2) we compare the KNO distributions of the two samples and one can indeed see how the distribution of jetty events shows much less fluctuations around z=1, a situation close to that found in e^+e^-. In figs.(3a) and (3b) one can see that the average transverse momentum of inclusive pions is higher for the jetty events than for the rest of the sample and that the separation into two samples has either eliminated altogether the multiplicity dependence (jetty events) or very much reduced it (non-jetty events).

The analysis, whose preliminary results have been summarized above, points to the validity of the hypothesis of a sizable jet-contamination in minimum bias events. In the next section we shall try to describe a simple phenomenological model which incorporates the main idea of this talk, i.e. that first order QCD corrections to the bulk of multiparton scattering are responsible at least in part for the phenomena described in fig.(1).

3. Two Component Model

The simplest way to study the relationship between KNO scaling violations and the growth of $< p_t >$ with multiplicity is to separate the cross-section into two parts, as shown graphically in fig.4. Correspondingly, one can write :

$$\sigma_{tot}(s) = \sigma_0(s) + \sigma_1(s) \tag{1}$$

$$\frac{d\sigma(s)}{dn} = \frac{d\sigma_0(s)}{dn} + \frac{d\sigma_1(s)}{dn} \tag{2}$$

and

$$\frac{d\sigma(s)}{dndp_t} = \frac{d\sigma_0}{dn}P_0(p_t) + \frac{d\sigma_1}{dn}P_1(p_t) \tag{3}$$

In eqs.(2) and (3), $\frac{d\sigma_i}{dn}$ represent the inclusive n-particle cross-sections and $P_i(p_t)$ the normalized single particle transverse momentum distribution in a given n-inclusive process.

Within the above approximation, we can say that low-p_t physics, for which KNO scaling is supposed to hold and for which the transverse momentum distribution does not show any multiplicity dependence, is the one described by the first term at the right hand side of the above equations. The "new" effects can then be considered to arise from the second term. In the following we shall first discuss a model for the KNO function derived from soft QCD bremmstrahlung. We shall also show how this function can be approximated by the well known gamma distribution. The latter is one of the limits of the negative binomial distribution, introduced by Carruthers and Shih [17]to describe, among other physical phenomena, the multiplicity distribution and used by the UA5 Collaboration to fit the KNO function in various rapidity intervals[18]. We shall then use the soft QCD bremsstrahlung model in conjunction with eq.(2) to describe KNO scaling violations at the collider. We shall subsequently use the approximation given by the gamma- distribution to fit the preliminary UA1 data for multiplicity in the central region. Using eqs.(2) and (3), one then obtains the curves shown in figs. (2) and (6).

In the soft QCD bremsstrahlung model[19], the shape of the KNO function is obtained from that of the soft QCD radiation emitted in the scattering of quarks and gluons. By summing all soft massless quanta emitted in the collision one obtains the following expression for the energy distribution of the emitted radiation :

$$\frac{dP}{d\omega} = \int \frac{dt}{2\pi} e^{i\omega t - h(E,t)} \tag{5}$$

where

$$h(E,t) = \int_0^E \frac{d^3\underline{k}}{2k} |j_\mu(k)|^2 (1 - e^{-ikt}) \tag{6}$$

and

$$|j_\mu(k)|^2 = \frac{2\alpha_s(k_\perp)}{\pi^2 k_\perp^2}$$

The parameter E represents the maximum energy which a single soft gluon can carry away in a given parton-parton collision. Assuming that on the average the final state pions equally share the radiated energy, we made the substitution

$$\omega = n < energy >_{single\ pion}$$

so as to obtain for the KNO function the expression

$$\Psi(\frac{n}{<n>}) = \beta(s) \int \frac{dt}{2\pi} e^{iz\beta(s)t - \beta(s)\int_0^1 \frac{dk}{k}(1-e^{-ikt})} \tag{7}$$

The parameter $\beta(s)$ which appears in the above expression is an effective soft gluon spectrum which incorporates the averaging process which takes place when eq.(5) is integrated between initial parton densities and final hadron fragmentation. To wit, we have written

$$< dP(\omega, E) >= d < \frac{\omega}{E} > \int \frac{dt}{2\pi} e^{i<\frac{\omega}{E}>t - <h(t)>} \tag{8a}$$

with

$$< h(t) >= \beta(s) \int_0^1 \frac{dk}{k}(1 - e^{-ikt}) \tag{8b}$$

and the symbol <> indicates the above mentioned average. We expect the effective parameter $\beta(s)$ to have a residual $\log\log s$ dependence as well as to be proportional to the color factors $c_F(= \frac{4}{3})$ or $c_A(= 3)$ according as to whether the emitting partons were quarks or gluons. A model which incorporates scaling violations of the type observed by the UA5 Collaboration can be constructed [20]by assuming that at low energy the dominant mechanism of particle production is through gluon radiation from quarks, and that only at high energy, i.e. past ISR and beyond, the contribution of gluon radiation from gluons starts becoming important. Although at present, this is strictly only a convenient model and nothing more, this subdivision may reflect the fact that for bremsstrahlung to take place in a significant way, the emitting gluons must be energetic and in a large amount. This means that one needs the fraction of energy x carried by the gluon to be small enough to correspond to a large density, but the energy of the emitting gluons to be large enough to allow the radiation of other gluons. This is so that α_s can be small enough for QCD effects to take place in lieu of particle production. In other words, we start by assuming that all gluons, soft and hard, are emitted by quarks. If the energy of the gluons is small enough that α_s is still in the confining phase, then these gluons will direcly hadronize. Thus the relevant mechanism of particle production is, as we said, through gluons emitted by quarks. If on the other hand the gluons are energetic enough that α_s is in the perturbative region, then these gluons can interact perturbatively with other gluons or quarks and thus can start bremsstrahlung on their own. From this latter bremsstrahlung process, characterized by the triple gluon coupling, there arises a mechanism of particle production which becomes important only at high energy, when the density of hard, low-x, gluons becomes large. With this model in mind, one can then approximately interpret the two terms at the right hand side of eq.(2) as one dominated by quark bremsstralung and the second dominated by gluon bremsstrahlung.

We can now construct the KNO function which incorporates all the above remarks. This function is obtained as the sum of two components, each one of them chracterized by a different average multiplicity $< n_i >$ and a different effective spectrum β_i. Using eqs.(2) and (7), one has

$$\Psi(z,s) = \frac{\Phi_0(\frac{n}{<n_0>}) + r\Phi_1(\frac{n}{<n_1>})}{1+r} \tag{9}$$

with

$$r(s) = \frac{\sigma_1(s)}{\sigma_0(s)}$$

and

$$\Phi_i = < n > \frac{1}{\sigma_i(s)} \frac{d\sigma_i(s)}{dn} \tag{10}$$

$$= \frac{< n >}{< n_i >} \beta_i(s) \int \frac{dt}{2\pi} e^{i\beta_i(s)\frac{n}{<n_i>}t - \beta_i \int_0^1 \frac{dk}{k}(1-e^{-ikt})}$$

One also has

$$< n(s) > = \frac{< n_0(s) > + r(s) < n_1(s) >}{1 + r(s)}$$

The number of parameters can be reduced by using the known ratio of the color factors $\frac{c_A}{c_F} = \frac{9}{4}$. According to the interpretation we just put forward for the two terms in eq.(2), we would write

$$\frac{\beta_0(s)}{\beta_1(s)} \approx \frac{c_F}{c_A} \approx \frac{< n_0 >}{< n_1 >} \tag{11}$$

By fixing $\beta_0(s) = 2.5$ at ISR (from the dispersion) and evolving to the collider energy, we find[20] that a good fit to the UA5 data[2] can be obtained if the fraction of events produced through the triple gluon coupling is as large as 12%. We show our fit in fig.5.

We now turn to discuss the UA1 data[3,16]. As mentioned before, we find that, from the point of view of doing numerical calculations, the bremsstrahlung distribution of eq.(7) is not very convenient. We then resort to approximate eq.(8b) as follows :

$$< h(t) > \approx b \log[1 + it]$$

which, after some simple manipulations, leads to

$$\Psi(z) \approx \frac{b}{\Gamma(b)}(bz)^{b-1}e^{-bz} \tag{12}$$

A numerical comparison between eqs.(12) and (7) shows that the two distributions have the same shape for $b \approx 2\beta(s)$. From here on we shall use the gamma distribution obtained above, instead of the actual bremsstrahlung shown in fig.5.

The UA1 data[16] for the multiplicity distribution cover a restricted rapidity interval, $|\eta| < 2.5$. For this set of data and in particular for the no-jet sample, we find that a good fit is provided by the gamma distribution with b=3.45. Then, according to the bremsstrahlung model, the KNO distribution relative to the jet sample should be obtained by making the substitution

$$\frac{b_{jetty}}{b_{no-jets}} = \frac{9}{4} = \frac{< n_{jetty} >}{< n_{no-jets} >}$$

In figs.(2a,b) we show the fit to the no-jet and jet sample with the parameters thus determined. It does appear that the simple ansatz of eq.(11) represents the data quite well.

The same ansatz can then be used to descrive the growth of $< p_t >$ with multiplicity. From eqs.(2,3) one has

$$< p_t >= \frac{< p_t >_0 \Phi_0(\frac{n}{<n_0>}) + r(s) < p_t >_1 \Phi_1(\frac{n}{<n_1>})}{\Phi_0(\frac{n}{<n_0>}) + r(s)\Phi_1(\frac{n}{<n_1>})}$$

Fixing the fraction of jetty events to be $r = 0.12$ and the average $< p_t >' s$ from the data, $< p_t >_{no-jets}= 385\ MeV/c^2$ and $< p_t >_{jets}= 500\ MeV/c^2$, one obtains the curve shown in fig. (6). Notice that to describe these data, one needs a value $< n_0 >= 13$, which is somewhat lower than the one characterizing the multiplicity data. This can be justified, by noticing that fig.(3a) definitely indicates a residual jet contamination in the no-jet sample.

The fits can be improved if a three component model is used : such a model could include, in addition to the quark-quark and gluon-gluon scattering terms, a mixed term corresponding to quark-gluon scattering. The correspondance between the data and the phenomenological curve would improve , but the number of parameters would increase as well. It is then necessary at this point to start a direct comparison between the data and QCD prediction for hard parton-parton scattering. In the next section, we shall report on such a calculation.

4. QCD Contribution to the Inelastic Cross-Section

In 1973, a suggestion[21] was made that the observed rise of the total cross-section at the ISR could be attributed to hard parton-parton collisions. Subsequent calculations of the QCD cross-section could neither confirm nor exclude this ansatz, the reason being that the jet cross-section is singular at $t = 0$ and its integrated value depends upon the minimum p_t of the jets[22]. There is thus a theoretical uncertainty which reflects the transition from a many body interaction type regime to the perturbative area. Recent results at the collider concerning the total cross-section have confirmed the rise in a very dramatic way. We shall now evaluate the QCD contribution to the rise of the total cross-section and compare this value with that obtained by the preliminary UA1 analysis mentioned in sect.2. For such a comparison with theoretical expectations, we are interested in the overall QCD contribution when the minimum transverse momentum of the partons is 5 GeV. At the collider, such a transverse momentum corresponds to $x_T \approx 0.02$, for which value the dominant contribution is from gluon-gluon scattering. An order of magnitude estimate can easily be obtained by using the small angle limit for the various scattering amplitudes[22], i.e. we can write

$$\sigma^{jet} = \frac{\pi\alpha_s^2}{2s}\int_{\tau_0}^{1}\frac{d\tau}{\tau^2}\mathcal{F}(\tau)\int_{-z_0}^{+z_0} dz^*\,|\mathcal{A}(z^*,\tau)|^2$$

with

$$\mathcal{F}(\tau) = \int_{\tau}^{1}\frac{dx}{x}F(x,Q^2)F(\frac{\tau}{x},Q^2)$$

and

$$|\mathcal{A}(z^*,\tau)|^2 = \frac{9}{8}\frac{(3+z^{*2})^3}{(1-z^{*2})^2}$$

The limits of integration z_0 and τ_0 depend upon the minimum allowed value for the p_t of the partons. To wit, we have

$$2p_{t_{min}} = \sqrt{s\tau_0} = \sqrt{s\tau(1-z_0^2)}$$

Using UA1 parton densities[23],i.e.

$$F(x,Q^2) = G(x,Q^2) + \frac{4}{9}(Q(x,Q^2) + \bar{Q}(x,Q^2)) = 6.2\ e^{-9.5x} \qquad at\ Q^2 = 2000\ GeV^2$$

$\alpha_s = 0.3$ and $p_{t_{min}} = 5\ GeV$, one obtains an integrated inelastic cross-section of 3 mb, not very far from the preliminary UA1 results on the mini-jets ($10 \div 15\%$ of σ_{NSD}). Thus the experimental results are in reasonable agreement with QCD predictions on low-x jet production. Concerning the s-dependence of the cross- section, it is worth noting that gluon-gluon scattering is characterized by a $\ln^2 s$ growth. This is similar to the well known case of $\gamma\gamma$ scattering in e^+e^- processes.

To proceed in the QCD analysis of the mini-jet sample, one must study the p_t and E_T-distribution of the sample. The calculation of the total scalar E_T comes from two sources : final state fragmentation and initial state bremsstrahlung accompanying the hard parton-parton scattering process, on the one hand, and bremsstrahlung from the rest of the event, on the other. In fact, unlike the p_t-distribution of the jets, the variable scalar E_T directly reflects the hermeticity of the UA1 detector, and thus it measures not only the hard parton scattering process but also the *debris* which result from the breaking up of the proton when a hard parton is emitted. We refer to this as the underlying event(UE). The contribution of the underlying event to this type of measurement when jet production occurs, can be observed if one plots the transverse energy flow around the jet axis[16]. These figures indicate that away from the jet there is a constant "floor", which points to an isotropic distribution. One can see that the jet profile stand out less and less as the jet trigger is lowered, reflecting the experimental difficulty of detecting low E_T jets. The effect of the underlying event can be incorporated by writing the following expression for the total scalar transverse energy measured in a jet event :

$$\frac{d\sigma}{dE_T} = \sum_{ij} \int dE\ P_{ij}^{UE}(E_T - E)\frac{d\sigma_{ij}^{jet}}{dE} \tag{13}$$

where P_{ij}^{UE} represents the normalized E_T distribution of the underlying event while $\frac{d\sigma_{ij}^{jet}}{dE}$ is the E_T distribution from bremsstrahlung and fragmentation accompanying the hard scattering.The subscript ij indicates the contribution from various types of partons and reflects the possibility that the underlying event be correspondingly different. A model for scalar E_T distribution at the collider has been advanced by M.Greco[24]. Here we examine only the case when a hard process has taken place. Referring to the hard process shown in fig.4b, the differential transverse energy cross-section is written as

$$\frac{d\sigma^{naive}}{dE_T} = \frac{\pi E_T}{2s^2}\sum_{ijkl}\int\frac{d\tau}{\tau^3}\int_\tau^1\frac{dx}{x}F_i(x,Q^2)F_j(\frac{\tau}{x},Q^2)\frac{\alpha_s^2(E_T)}{\sqrt{1-\frac{E_T^2}{s\tau}}}\left|\mathcal{A}(\tau,E_T^2)\right|^2_{ijkl}$$

$$= \sum_{ijkl} \int \frac{d\tau}{\tau} \mathcal{F}_{ij}(\tau, Q^2) \frac{d\sigma^{QCD}_{ijkl}}{dE_T} \tag{14}$$

To include initial state bremsstrahlung, eq.(14) is modified so as to obtain the following expression :

$$\frac{d\sigma^{jet}_{ij}}{dE_T} = \sum_{kl} \int_{\tau_0}^{1} \frac{d\tau}{\tau} \mathcal{F}_{ij}(\tau, Q^2) \int_{E_0}^{E_T} dE' P_{ij}(E_T - E') \frac{d\sigma^{QCD}_{ijkl}}{dE'} \tag{15}$$

with the soft bremsstrahlung distribution given by[25]

$$P(\omega) = \frac{1}{\pi} \int_0^{\infty} dt e^{-A(t,\omega_{mx})} B(t, \omega_{mx}, \omega) \tag{16}$$

with

$$A(t, \omega_{mx}) = c_{ij} \frac{4}{\pi} \int_0^{\omega_{mx}} \frac{dk_\perp}{k_\perp} \alpha_s(k_\perp) \log(\frac{2\omega_{mx}}{k_\perp})(1 - cosk_\perp t)$$

and

$$B(t, \omega_{mx}, \omega) = cos\left(\omega t - c_{ij} \frac{4}{\pi} \int_0^{\omega_{mx}} \frac{dk_\perp}{k_\perp} \alpha_s(k_\perp) \log(\frac{2\omega_{mx}}{k_\perp}) sin(k_\perp t)\right)$$

A close inspection of eq.(16) shows that the bremsstrahlung distribution for the E_T variable is very close in form to that which we used for the soft gluon radiation and which led to the KNO function. This is an obvious consequence of the fact that in either cases, one is summing over all soft gluon emission diagrams, but with respect to different variables (energy vs. *transverse* energy). As we discussed previously for the bremsstrahlung model, these bremsstrahlung distributions vary according as to the type of emitting partons involved. This is reflected in the coefficients c_{ij} which are defined as

$$c_{qq} = c_F = \frac{4}{3}, \qquad c_{gg} = c_A = 3, \qquad c_{qg} = \frac{1}{2}(c_F + c_A) = \frac{13}{6}$$

In the above expressions, the quantity ω_{mx} represents the maximum transverse momentum allowed to a single gluon emitted in the process and it is the exact (transverse) analogue of the parameter E which appeared in the energy distribution. Energy-momentum conservation in eq.(15) suggests

$$\omega_{mx} = \sqrt{(s\tau)} - E'$$

Finally, the bremsstrahlung corrected hard cross-section of eq.(15) has to be folded with the E_T distribution of the underlying event. While the QCD calculation, although plagued by a number of uncertainties like gluon density and the value for Λ, is along a well trodden path, the question of what to choose for the underlying event is quite open. In principle, the underlying event is different for different parton types and it has a functional dependence upon the parton densities. In practice, these differences are smoothed down by

the many integration processes taking place so that we can simply use an E_T distribution independent of the parton densities. This is the simplification adopted in writing eq.(13), which corresponds to use a distribution averaged over the densities. As for the specific form, one can take this function to be described by a bremsstrahlung type distribution, i.e. we write

$$P(E_T) = \frac{1}{< E_T >_{UE}} \frac{b}{\Gamma(b)} \left(b \frac{E_T}{< E_T >_{UE}} \right)^{b-1} e^{-b \frac{E_T}{< E_T >_{UE}}}$$

with the choice of the two parameters b and $< E_T >_{UE}$ which depend upon the type of partons involved in the hard scattering. Numerical calculations are in progress and will be presented elsewhere.

4. Conclusion

We have discussed the importance of low-x hard parton scattering in minimum bias events and pointed out its connection to both KNO scaling violations as well as to the observed growth of $< p_t >$ with multiplicity in inclusive pion distributions. The contribution of these mini-jets to the total cross-section has been calculated and a model for the transverse energy distribution characterizing any event accompanied by jets has been presented.

References

1. M.Jacob, Proceedings of the SLAC Topical Conference, 27-29 July 1983 ; G.Pancheri and C.Rubbia,Nuclear Physics *A*418,117c (1984). G.Pancheri and Y.N.Srivastava, Proceedings of the APS-DPF Meeting, October 31 - November 3, Santa Fe, New Mexico, 1984.
2. K.Alpgard et al., Physics Lett. 121*B*,209 (1983) ; G.J.Alner et al., Physics Lett.138*B*,304 (1984). UA5 Collaboration.
3. G.Arnison et al.,Physics Lett. 118*B*,167 (1982). UA1 Collaboration.
4. R.Battiston et al., Physics Letters 117*B*,126 (1982). UA4 Collaboration. G.Arnison et al.,Physics Letters 128*B*,336 (1983). UA1 Collaboration.
5. W.Thome' et al., Nuclear Physisc *B*129,365 (1977); A.Breakstone et al.,Physical Review *D*30,528(1984).
6. K.Alpgard et al., Physics Letters 107*B*, 310 (1981). UA5 Collaboration. G.Arnison et al., Physics Letters 107*B*,320 (1981). UA1 Collaboration.
7. R.V.Gavai and H.Satz, Physics Letters 112*B* 413 (1982).
8. Z.Koba,H.Nielsen and P.Olesen, Nuclear Physics*B*40,317 (1972).

9. T.Ekelof, in Proceedings of the International Europhysics Conference on High Energy Physics, Brighton, July 1983.
10. C.M.G.Lattes et al.,Physics Reports 65,151 (1980).
11. For a review of theoretical and phenomenological interpretations : G.Pancheri, "Hadronic Multiplicity Distributions and KNO Scaling Violations", Proceedings of the *XV International Symposium on Multiparticle Dynamics*, Lund, Sweden, 10-16 June,1984. Ed. by G.Gustafson and C.Peterson.
12. L.Van Hove, Physics Letters 118*B*,138 (1982).
13. S.Barshay, Physics Letters 127*B*,129 (1983).
14. A.Capella, A.Staar and J.Tran Thanh Van, Proceedings of the Rencontre de Moriond, March 1984.
15. M.Biyajima, Physics Letters 137*B*,225 (1984); ibid.139*B*,93 (1984).
16. G.Ciapetti, these Proceedings.
17. P.Carruthers and C.C.Shih, Physics Letters 127*B*, 242 (1983).
18. G.Ekspong, these Proceedings.
19. G.Pancheri and Y.Srivastava,Physics Lett.128*B*, 433 (1983).
20. G.Pancheri,Y.Srivastava and M.Pallotta,Physics Letters 15*B*,453 (1985).
21. D.Cline, F.Halzen and J.Luthe, Physical Review Letters 31,491 (1973).
22. F.Halzen, "QCD Collider Physics", Proceedings of the *XV International Symposium on Multiparticle Dynamics* Lund, Sweden 10-16 June 1984. Ed. by G.Gustafson and C.Peterson. T.Gaissner and F.Halzen, Physical Review Letters 54, 1754 (1985).
23. G.Arnison, Physics Letters 136*B*,294 (1984).
24. M.Greco, Nucl.Physics *B*250,450 (1985).
25. F.Halzen, A.D.Martin, D.M.Scott and M.P.Tuite, Z.Phys. *C*14,351 (1982).

Figure Captions

Figure 1. : (1a) Moments of the KNO function as a function of energy. Data are from ref.[2] ; (1b) Total cross-section as a function of energy. Data compilation from ref.[9] ; (1c) Growth of average transverse momentum in inclusive pion distributions. Data are from UA1 collaboration[3] and ABCDHW Collaboration[5].

Figure 2. : (2a) KNO distribution of minimum bias no-jet events (see text). UA1 1983 Data[16] ; (2b) KNO distribution of jet ($E_T > 5\ GeV$) sample (see text). UA1 1983 Data [16]. Fits are from two component bremsstrahlung model described in the text.

Figure 3. : (3a) Mean Transverse momentum of no-jet sample (see text). UA1 1983 Data [16] ; (3b) Mean Transverse momentum of jet sample ($E_T > 5\ GeV$). UA1 1983 Data[16]. For all UA1 Data, the pseudorapidity is $|\eta| < 2.5$.

Figure 4. : Decomposition of the cross-section into non-perturbative and perturbative (order α_s) component.

Figure 5. : Corrected UA5 Multiplicity Data from 1981 and 1982 run at the Cern $S\bar{p}pS$ Collider. The continuous curve is obtained from the two component soft QCD bremsstrahlung model described in the text.

Figure 6. : UA1 1983 Data[16]. Growth of inclusive single pion $< p_t >$ as a function of multiplicity. The continuous curve is based on the two component model described in the text, using same set of parameters as for the fits to the KNO function shown in fig.(2a,b).

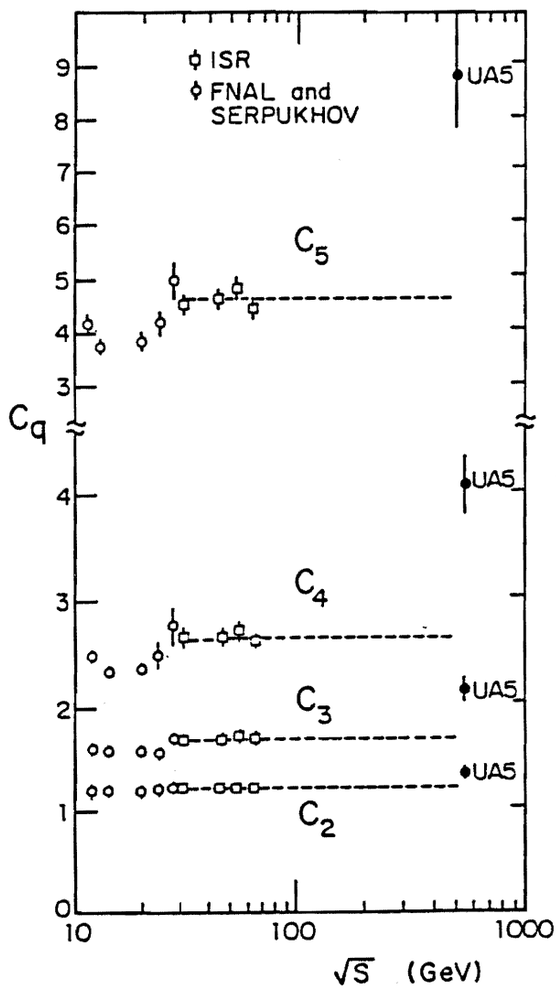

Fig. 1a

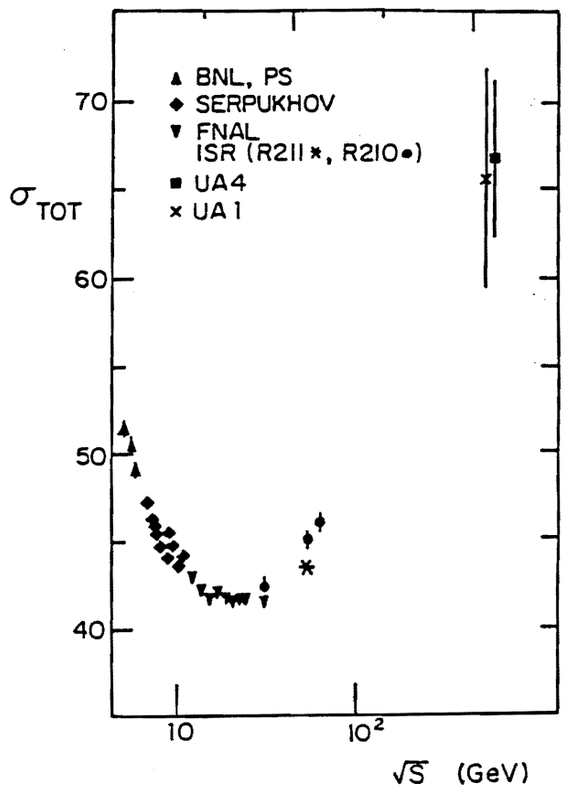

Fig. 1b

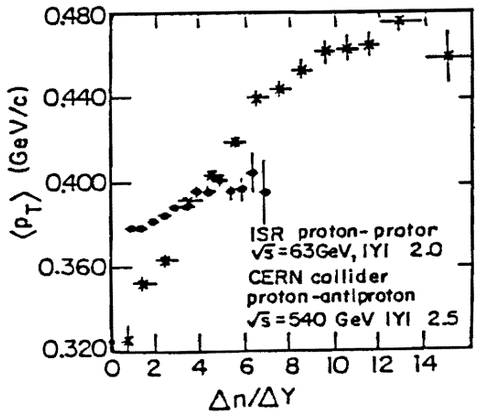

Fig. 1c

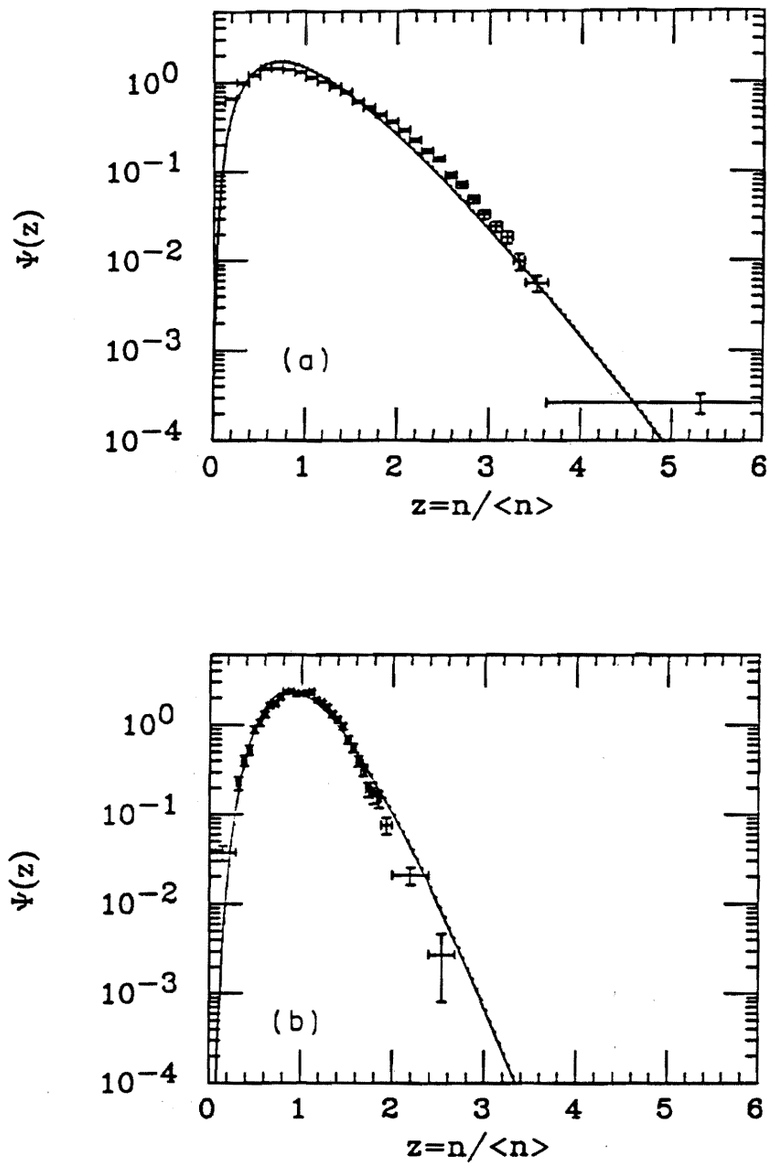
Ψ(z)
10^0
10^-1
10^-2
10^-3
10^-4
(a)
0 1 2 3 4 5 6
z=n/<n>
Ψ(z)
10^0
10^-1
10^-2
10^-3
10^-4
(b)
0 1 2 3 4 5 6
z=n/<n>

Fig. 2

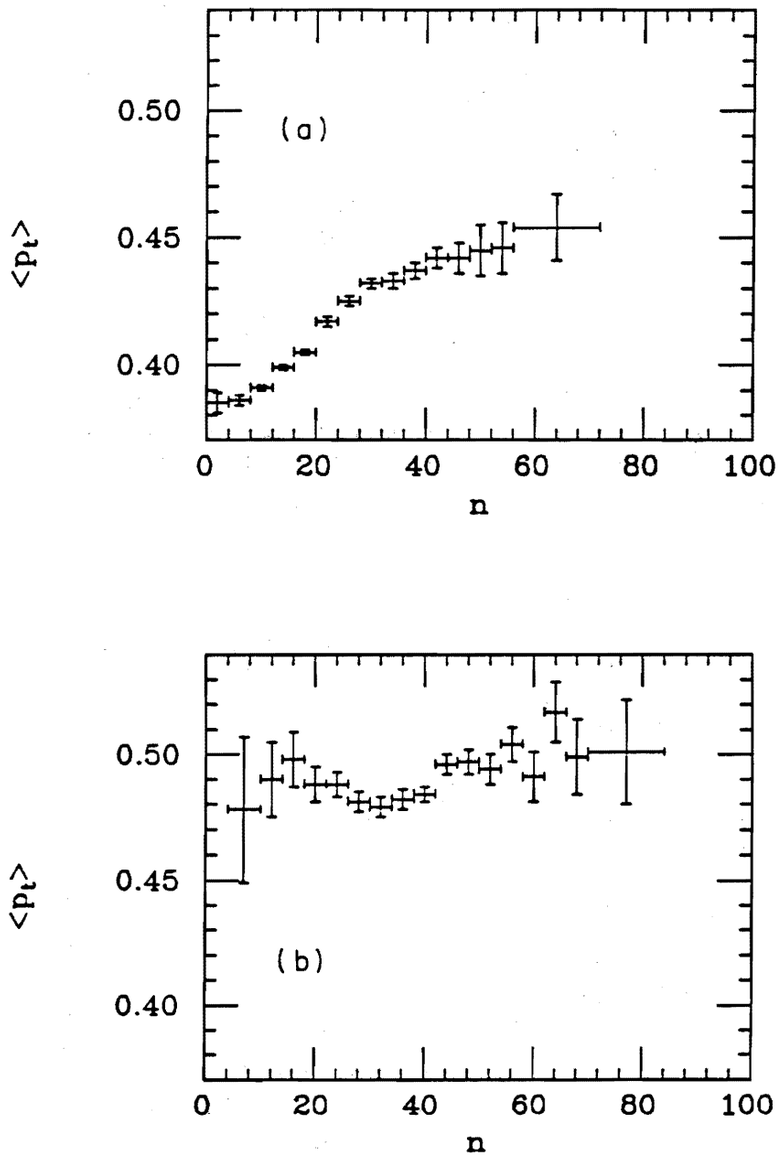
0.50
0.45
0.40
<p_t>
(a)
0
20
40
60
80
100
n
0.50
0.45
0.40
<p_t>
(b)
0
20
40
60
80
100
n

Fig. 3

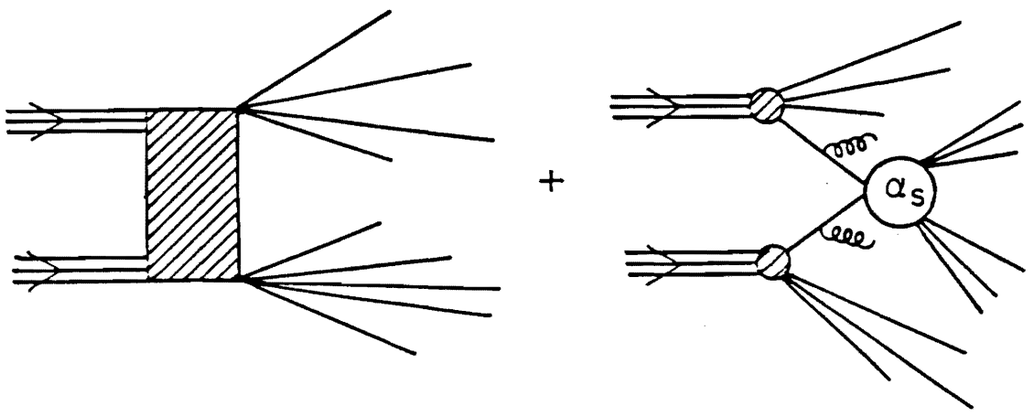

Fig. 4

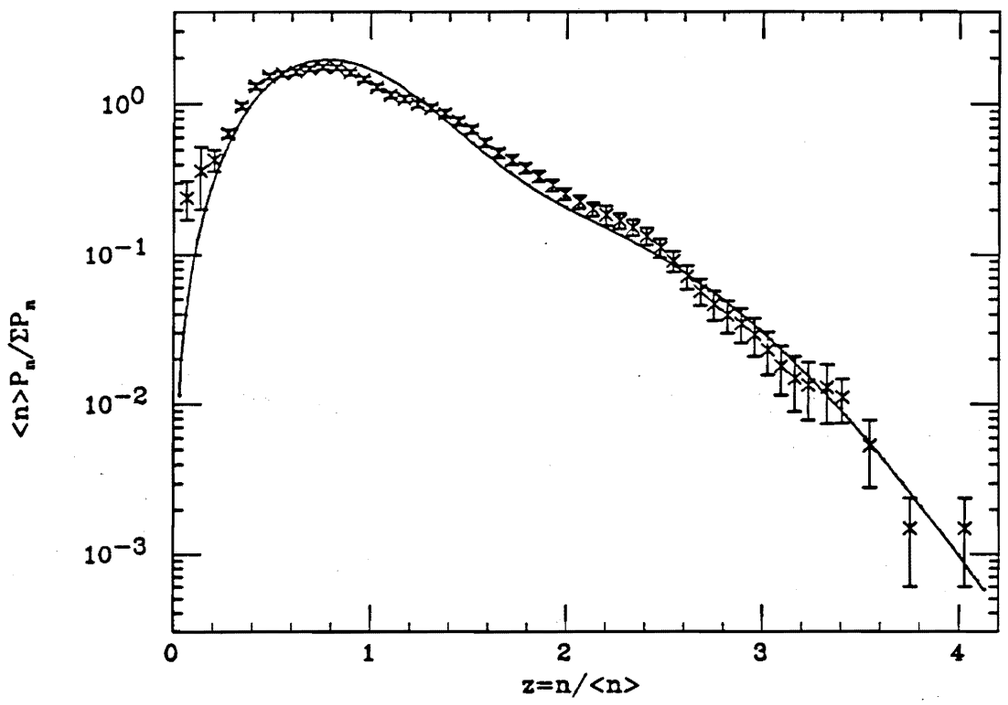
10^0
10^{-1}
10^{-2}
10^{-3}
$\langle n \rangle P_n / \Sigma P_n$
0
1
2
3
4
$z = n/\langle n \rangle$

Fig. 5

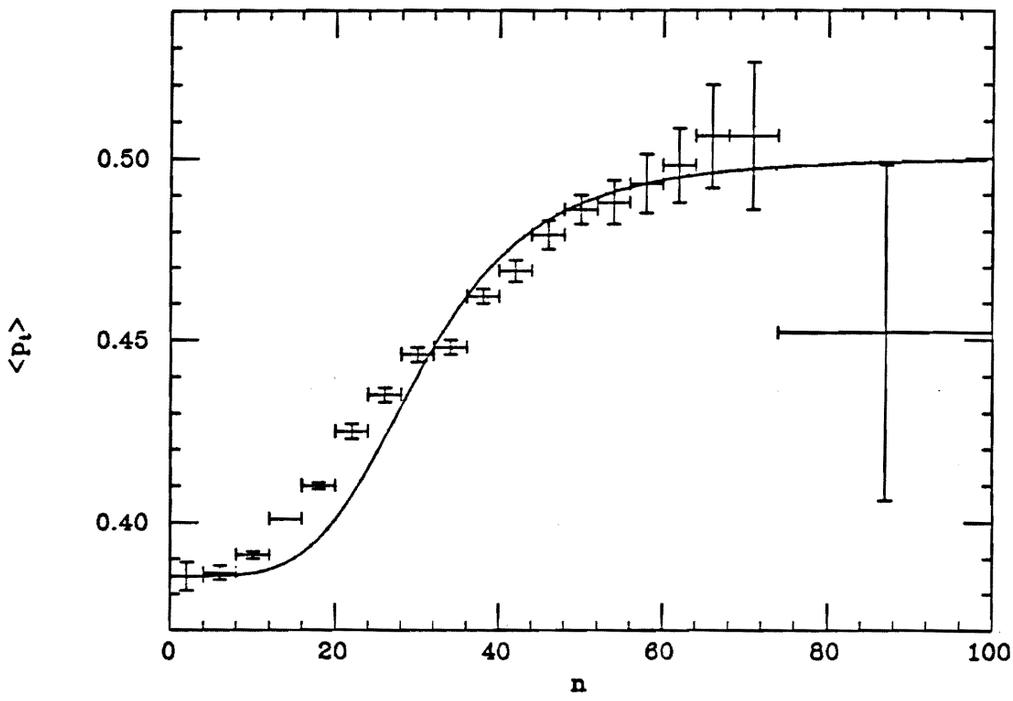

Fig. 6